Circuits Syst Signal Process (2016) 35:1973–1982
DOI 10.1007/s00034-015-0222-2

Approximated Fractional-Order Inverse Chebyshev Lowpass Filters

Todd J. Freeborn[1] · **Ahmed S. Elwakil**[2] · **Brent Maundy**[3]

Received: 6 June 2015 / Revised: 8 December 2015 / Accepted: 9 December 2015 /
Published online: 22 December 2015

Abstract In this paper we use a least-squares fitting routine to approximate the stop-band ripple characteristics of fractional-order inverse Chebyshev lowpass filters which have fractional-order zeros and poles. MATLAB simulations of $(1+\alpha)$-order lowpass filters with fractional steps from $\alpha = 0.1$ to $\alpha = 0.9$ are given as examples. SPICE simulations of 1.2-, 1.5-, and 1.8-order lowpass filters and experimental results of a 1.5-order filter using approximated fractional-order capacitors in a Multiple-Input Biquad circuit validate the implementation of these circuits.

Keywords Fractional-order circuits · Fractional-order filters · Analog filter circuits · Fractional calculus

1 Introduction

The field of fractional-order circuits refers to electrical circuits incorporating concepts from fractional calculus into their design and realization [5]. This import introduces a further element of flexibility during their design. When applied to electronic filters for

✉ Ahmed S. Elwakil
elwakil@ieee.org

Todd J. Freeborn
tjfreeborn1@eng.ua.edu

Brent Maundy
bmaundy@ucalgary.ca

1 Department of Electrical and Computer Engineering, University of Alabama, Tuscaloosa, USA

2 Department of Electrical and Computer Engineering, University of Sharjah, Sharjah, United Arab Emirates

3 Department of Electrical and Computer Engineering, University of Calgary, Calgary, Canada

signal processing, the field of fractional-order filter circuits emerged [12,13]. This field has focused on theory [1,11,17], implementation [3,16,18], and applications [19] of filters with magnitude characteristics not easily realizable using integer-order circuits. While traditional filters typically yield $-20n$ dB/decade stopband attenuations (where n is the filter integer order), fractional-order filters provide more precise control with $-20(n+\alpha)$ dB/decade attenuations, where $0 \leq \alpha \leq 1$ is the fractional-component of the order. These concepts also provide alternative design methodologies for the realization of asymmetric band-pass [2] and band-reject [10] filters with high-quality factors.

Filter circuits are typically designed using their transfer functions rather than their time domain representations, which also remains true when designing them using fractional-order concepts. Whereas integer-order filters use the integer-order Laplacian operator, s, fractional-order filters use the Laplacian operator raised to power α yielding s^{α}, which is referred to as the fractional Laplacian operator.

Lowpass $(1+\alpha)$-order fractional transfer functions have previously been explored to realize approximated Butterworth [7] and Chebyshev [6] passband magnitude characteristics. These responses were both realized using the fractional transfer function

$$H_1^{1+\alpha}(s) = \frac{k_1}{s^{1+\alpha} + k_2 s + k_3} \tag{1}$$

where the coefficients $k_{1,2,3}$ were selected to optimize the responses over a select frequency band. However, while the Butterworth and Chebyshev approximations can be realized with all-pole transfer functions, the inverse Chebyshev and elliptic approximations require both poles and zeros. Therefore, it is required to explore further $(1+\alpha)$-order transfer functions with both poles and zeros. In this work, a $(1+\alpha)$-order transfer function is investigated to approximate the stopband ripple characteristics of inverse Chebyshev lowpass filters. The optimum coefficients required are determined using a nonlinear least-squares optimization routine. MATLAB simulations of the $(1+\alpha)$-order lowpass filters with fractional steps from $\alpha = 0.1$ to $\alpha = 0.9$ designed using this process are given as examples. Further, validation with SPICE simulations of 1.2−, 1.5-, and 1.8-order lowpass filters and experimental results of a 1.5-order filter realized using an approximated fractional-order capacitor in a multiple-input biquad (MIB) circuit are given.

2 Approximated Inverse Chebyshev Response

Inverse Chebyshev lowpass filters are generally realized using lowpass notch circuits described by the transfer function

$$H_2(s) = \frac{s^2 + k^2\omega_0^2}{s^2 + s\frac{\omega_0}{Q} + \omega_0^2} \tag{2}$$

where k^2 is the DC gain, ω_0 is the notch frequency, and Q is the quality factor. An example of a second-order inverse Chebyshev filter designed with a minimum loss of 50 dB is given by:

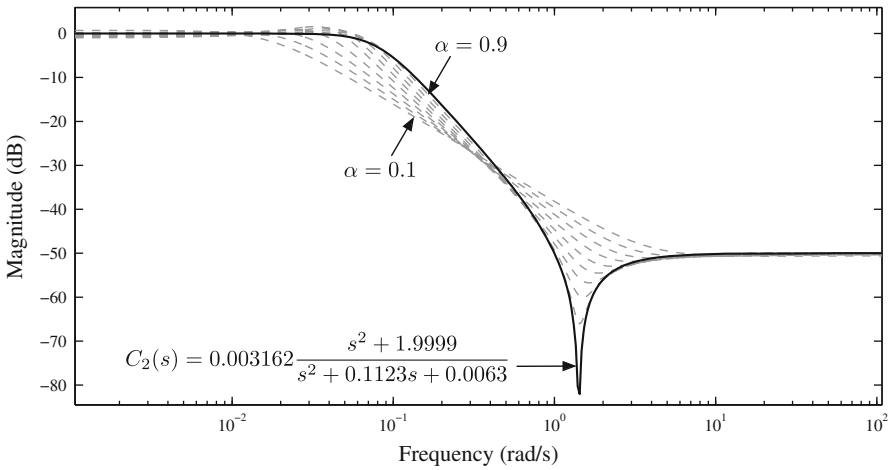

Fig. 1 Simulated magnitude responses of $(1+\alpha)$ lowpass fractional-order filter circuits for $\alpha = 0.1$ to 0.9 in steps of 0.1 with coefficients selected to approximate inverse Chebyshev stopband response

$$C_2(s) = 0.003162\frac{s^2 + 1.9999}{s^2 + 0.1123s + 0.0063} \tag{3}$$

The magnitude response of (3) is shown in Fig. 1 as a solid line with a DC gain of 1 ($0.003162 \times 1.9999/0.0063 \approxeq 1 = 0\,\text{dB}$) and high-frequency gain of $0.003162 \approxeq 50\,\text{dB}$. This response requires both poles and zeros differentiating it from the Butterworth and Chebyshev responses which only require poles in their realization. Similarly, a fractional-order lowpass notch filter requires both fractional poles and zeros with a $(1+\alpha)$-order transfer function which satisfies this requirement given by

$$H_3^{1+\alpha}(s) = a_4\frac{a_1 s^{1+\alpha} + 1}{a_2 s^{1+\alpha} + a_3 s^{\alpha} + 1} \tag{4}$$

This transfer function will have a notch-shaped magnitude response with low- and high-frequency gains of a_4 and $a_4 a_1/a_2$, respectively, and an attenuation from passband to stopband dependent on α, as shown in Fig. 1.

Realizing an approximated inverse Chebyshev response using (4) requires selection of coefficients $[a_1, a_2, a_3, a_4]$ that approximate the ripple behavior in the stopband of the magnitude response. The use of optimization routines in the design of fractional filters [6,9], provides a method to determine these coefficients. One implementation described in [6] used a nonlinear least-squares fitting that searches for the coefficients to minimize the squared error between the magnitude response of (1) and a second-order Chebyshev response over the frequency range $\omega \epsilon \left[10^{-5}, 10^{0}\right]$ rad/s. This process is applied here, modified to use the second-order inverse Chebyshev response and fractional notch transfer function given by (3) and (4), respectively, over the frequency band $\omega \epsilon \left[10^{-3}, 10^{3}\right]$ rad/s. This optimization problem is described by

$$\min_x \| \, |H(x,\omega)| - |C_2(\omega)| \, \|_2^2 = \min_x \sum_{i=1}^{k} (|H(x,\omega_i)| - |C_n(\omega_i)|)^2 \quad \text{s.t. } x > 0.1 \tag{5}$$

where x is the vector of filter coefficients, $|H(x)|$ is the magnitude response using (4) with x, $|C_2(j\omega)|$ is the second-order inverse Chebyshev magnitude response given by (3), and k is the total number of data points in the magnitude responses. The constraint is added to prevent the return of negative coefficients which are not physically realizable, as well as values that would be unrealistically small for a physical realization. The routine was implemented in MATLAB using the *lsqcurvefit* function with termination tolerances of the function value and the solution set to 10^{-6}.

The coefficients returned by this search are given in Table 1 for $\alpha = 0.1$ to 0.9 in steps of 0.1. The 50-dB ripple for the second-order inverse Chebyshev response was selected over smaller magnitudes to highlight the difference in ripple size using the fractional-order response over the integer-order response, but could be applied to any second-order inverse Chebyshev response.

The simulated magnitude responses using Table 1 coefficients in (4) are given in Fig. 1 as dashed lines. The slope of these responses in the frequency band from $\omega = 0.02$ to 10 rad/s decreases with increasing α, while the frequency that each response reaches -3 dB also decreases with increasing α; occurring at 0.022, 0.029, 0.038, 0.049, 0.06, 0.067, 0.073, 0.079, and 0.081 rad/s for $\alpha = 0.1$ to 0.9 in steps of 0.1, respectively. The minimum stopband magnitude is also impacted by the order, decreasing with decreasing order. The peak values are -41.4, -43.2, -45.2, -47.4, -49.8, -52.5, -55.6, -59.6, -66.0 dB for $\alpha = 0.1$ to 0.9 in steps of 0.1, respectively, when measured at $\omega = 1.415$ rad/s (the frequency at which $|C_2(\omega)|$ reaches its minimum). These responses highlight that the introduction of the fractional order increases the flexibility in shaping the magnitude response, increasing the potential control over the attenuation and ripple characteristics. In the following section, stability is analyzed to ensure these fractional transfer functions are physically realizable.

Table 1 Coefficient values for $(1+\alpha)$ fractional-order transfer functions to approximate iverse Chebyshev stopband response

Order	α	a_1	a_2	a_3	a_4	$\lvert\theta_W\rvert_{\min}$
$1+\alpha$	0.1	0.2392	91.20	0.1	1.1294	18.00°
	0.2	0.2793	94.69	0.1	1.033	16.46°
	0.3	0.3227	100.4	0.1	0.9676	15.11°
	0.4	0.3687	107.7	0.1	0.9211	13.94°
	0.5	0.4149	117.2	0.2251	0.8977	13.04°
	0.6	0.4540	134.8	1.6167	0.9485	12.99°
	0.7	0.4855	148.9	3.762	0.9799	13.05°
	0.8	0.5054	158.2	6.933	0.9973	13.28°
	0.9	0.5102	161.4	11.47	1.004	13.81°

2.1 Stability

To analyze the stability of fractional filters requires conversion of the s-domain transfer functions to the W-plane defined in [14]. This transforms the transfer function from fractional order to integer order to be analyzed using traditional analysis methods. This process can be broken down into the following steps:

1. Convert the fractional transfer function to the W-plane using the transformations $s = W^m$ and $\alpha = k/m$ [14],
2. Select k and m for the desired α value,
3. Solve the transformed transfer function for all poles in the W-plane and if any of the absolute pole angles, $|\theta_W|$, are less than $\frac{\pi}{2m}$ rad/s then the system is unstable, otherwise if all $|\theta_W| > \frac{\pi}{2m}$ then the system is stable.

Applying this process to the denominator of (4) yields the characteristic equation in the W-plane given by:

$$a_2 W^{m+k} + a_3 W^k + 1 = 0 \tag{6}$$

The roots of (6) for $\alpha = 0.1$ to 0.9 were calculated with $k = 1$ to 9, respectively, when $m = 10$. The minimum root angles, $|\theta_W|_{\min}$, for each case are given in Table 1 and are all greater than the minimum required angle, $|\theta_W| > \frac{\pi}{2m} = 9°$, confirming that each transfer function using the coefficients in Table 1 is stable and physically realizable.

3 Circuit Realization

The $(1+\alpha)$-order transfer function (4) can be physically realized using the MIB circuit, given in Fig. 2, when the capacitor C_2 is replaced with a fractional-order capacitor. A fractional-order capacitor is an element with impedance $Z_C = 1/s^\alpha C$ where C is the pseudo-capacitance with units F $s^{\alpha-1}$ and $0 \leq \alpha \leq 1$ is the order. This component derives its name from the order placing it between the traditional circuit elements of a resistor ($\alpha = 0$) and capacitor ($\alpha = 1$). The transfer function of the MIB circuit using the fractional-order capacitor for C_2 is given by:

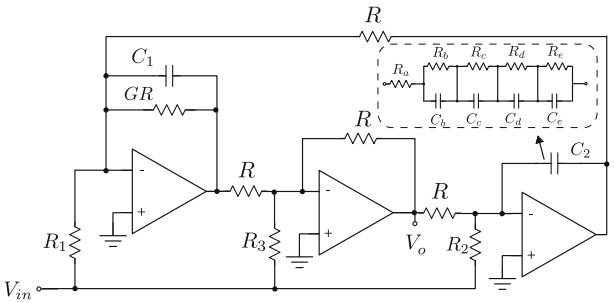

Fig. 2 Multiple-input biquad topology with RC ladder structure to realize a fourth-order integer approximation of a fractional-order capacitor given in subset

Table 2 Component values to realize (7) for the coefficients in Table 1 when $\alpha = 0.2, 0.5, 0.8$

α	C_1 (F)	C_2 (F $s^{\alpha-1}$)	R_1 (Ω)	R_2 (Ω)	R_3 (Ω)	R (Ω)	GR (Ω)
0.2	49μ	1.41μ	1.04 M	6.15 k	2.08 M	6.15 k	3.07 k
0.5	165μ	1.41μ	142 k	1 k	284 k	1 k	500
0.8	3.23μ	1.41μ	351 k	2.24 k	702 k	2.24 k	1.12k

$$H(s) = \frac{V_o(s)}{V_{in}(s)} = \frac{b_1 s^{1+\alpha} + b_2 s^{\alpha} + b_3}{s^{1+\alpha} + b_4 s^{\alpha} + b_5} \tag{7}$$

where $b_1 = R/R_3, b_2 = (1/R_3C_1G - 1/R_1C_1), b_3 = 1/C_1C_2R_2R, b_4 = 1/GC_1R, b_5 = 1/C_1C_2R^2$.

The values to realize the approximated fractional inverse Chebyshev responses are determined solving the system of equations formed by comparing the coefficients of (4) and (7). Solving for orders $(1 + \alpha) = 1.2, 1.5$, and 1.8 using the coefficients from Table 1 when the DC gain (a_4) is neglected, while setting $R_2 = R$, $R_1 = GR_3$, and $G = 0.5$ yields the scaled values given in Table 2. These values were scaled to realize realistic component values by applying a magnitude scaling $K_m = 1000$ and frequency scaling $K_f = 2000\pi$.

3.1 Approximated Fractional Capacitor

While significant progress has been achieved toward realizing fractional-order capacitors [4,8,15], there are currently no commercial devices available. Instead, integer-order approximations must be used to simulate and validate proposed fractional-order circuits. Multiple methods exist to design and realize these approximations which can be realized using either passive or active topologies. Based on collecting terms of a continued fraction expansion (CFE), we can realize an approximated fractional-order capacitor using an RC ladder network. This RC ladder network, when eight CFE terms are collected to yield a fourth-order approximation, is given in the subset of Fig. 2.

To realize approximations of 1.41 μF $s^{\alpha-1}$ fractional-order capacitors with orders 0.2, 0.5 and 0.8, respectively, the values in Table 3 are required. These values have been selected such that the frequency band around which the RC ladder is a good approximation is centered at 1 kHz. The impedance magnitude of the ideal (solid) and approximated (dashed) 1.41 μF $s^{\alpha-1}$ and fractional-order capacitor with order $\alpha = 0.5$ shifted to a center frequency of 1 kHz is presented in Fig 3. From this figure the approximation is very good over almost 4 decades, from approximately 200 Hz to 70 kHz.

Using the component values in Tables 2 and 3, the approximated fractional-order inverse Chebyshev lowpass filter was simulated in SPICE using LF411 op amps. The simulations realized $(1 + \alpha) = 1.2, 1.5$, and 1.8 responses which are given in Fig. 4 as dashed lines. For comparison, the ideal responses of (4) are also given as solid

Table 3 Component values to realize fourth-order approximations of $1.41\mu\text{F}\,\text{s}^{\alpha-1}$ fractional-order capacitors with $\alpha = 0.2$, 0.5, and 0.8

Component	Values		
	$\alpha = 0.2$	$\alpha = 0.5$	$\alpha = 0.8$
R_a (Ω)	11.9	991	53.1 k
R_b (Ω)	60	2.25 k	35.1 k
R_c (Ω)	152.8	3.38 k	29.7 k
R_d (Ω)	635.2 k	7.93 k	41.5 k
R_e (Ω)	34.4 k	65.8 k	125 k
C_b (F)	465 n	9.39 n	0.435 n
C_c (F)	904 n	33.2 n	3.05 n
C_d (F)	982 n	60.2 n	9.06 n
C_e (F)	422 n	77.9 n	22.8 n

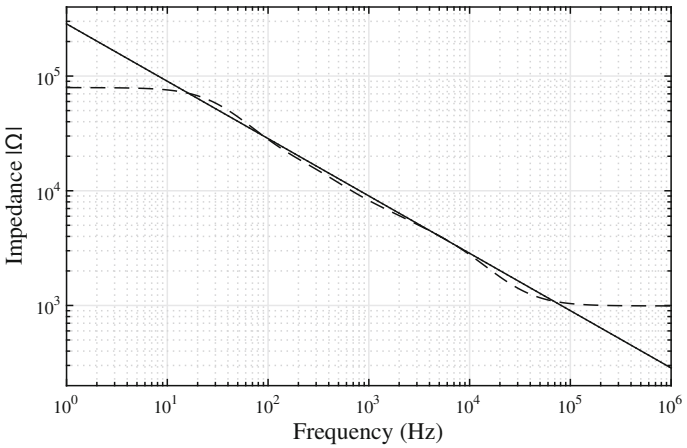

Fig. 3 Impedance magnitude of approximated fractional-order capacitor (*dashed*) compared to the ideal (*solid*) with pseudo-capacitance of $1.41\,\mu\text{F}\,\text{s}^{\alpha-1}$ with $\alpha = 0.5$ after scaling to a center frequency of 1 kHz

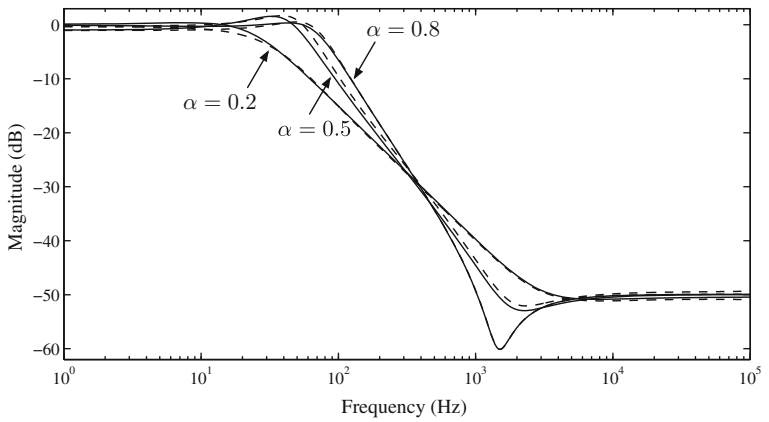

Fig. 4 PSPICE simulations using Fig. 2 compared to ideal simulations of (7) as *dashed* and *solid lines*, respectively, to realize approximated inverse Chebyshev lowpass filters of orders $(1 + \alpha) = 1.2$ and 1.5, and 1.8

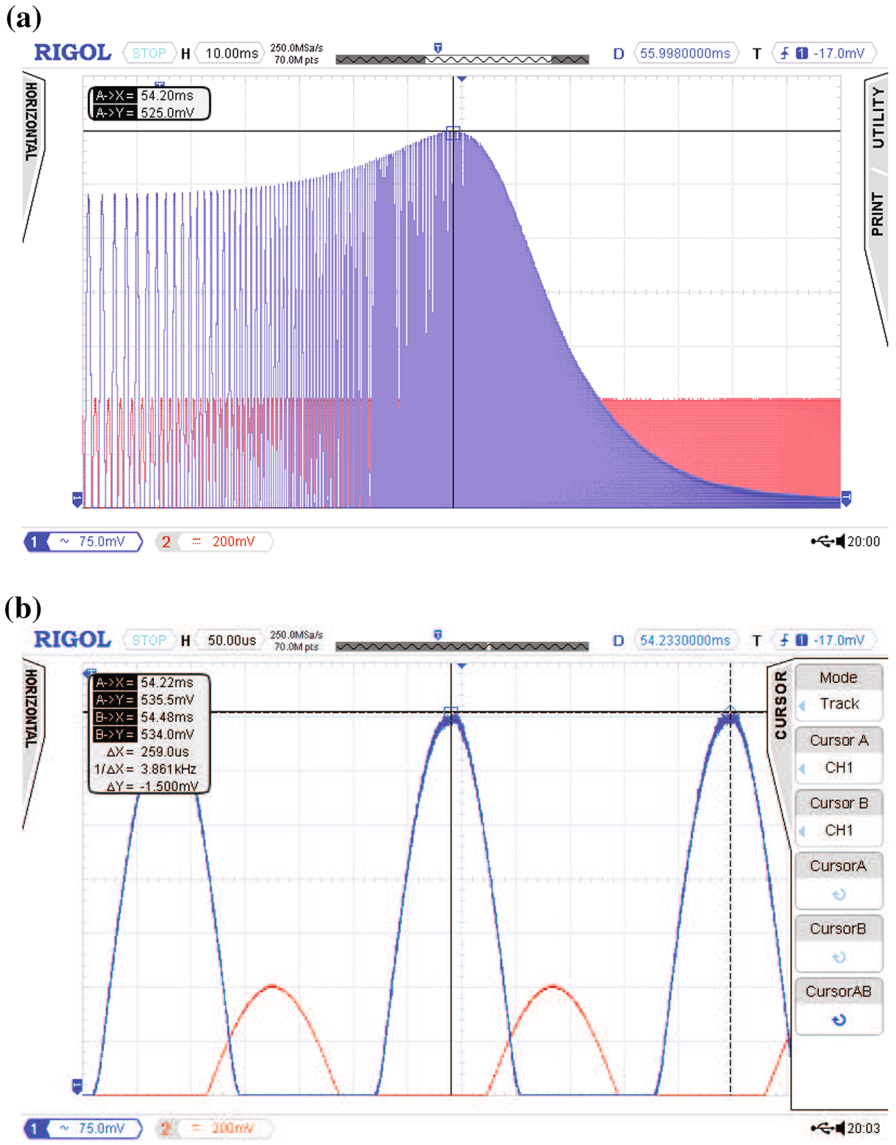

Fig. 5 Frequency response of Fig. 2 designed to realize an approximated inverse Chebyshev lowpass filter of order $(1+\alpha) = 1.5$ **a** frequency response and **b** zoom-in at the peak

lines. The SPICE results show good agreement with the ideal responses confirming the stopband ripples with a fractional-order step in the transition from passband to stopband. It should be noted that the SPICE simulations do deviate from the MATLAB simulated transfer function at low frequencies, because of the limited bandwidth of the fourth-order approximation of the fractional-order capacitor.

3.2 Experimental Results

The MIB circuit was physically realized to validate the proposed fractional-order lowpass filters. A 1.5-order ($\alpha = 0.5$) filter was implemented using AD844 op amps, which have a wider bandwidth than the LF411 op amps used for simulations. To take advantage of the larger bandwidth, design components were scaled to a frequency of 100 kHz as follows: $R = R_2 = 400\,\Omega$, $R_1 = 227\,\text{k}\Omega$, $R_3 = 113\,\text{k}\Omega$, $C_1 = 1\,\mu\text{F}$ and approximated fractional-order capacitor $C_2 = 1.4\,\mu\text{F}\,\text{s}^{\alpha-1}$ with $\alpha = 0.5$ when $G = 2$. The components to realize the approximated fractional-order capacitor were also scaled as: $R_a = 100\,\Omega$, $R_b = 225\,\Omega$, $R_c = 330\,\Omega$, $R_d = 800\,\Omega$, $R_e = 6.6\,\text{k}\Omega$, $C_b = 1$ nF, $C_c = 3.3$ nF, $C_d = 6$ nF, $C_e = 7.8$ nF. The response of this circuit to a sinusoidal input swept from 10 Hz to 100 kHz in 200 ms with amplitude 1 V is given in Fig. 5a. The attenuation in the stopband was measured as -9 dB/decade which is very close to the theoretical attenuation of -10 dB/decade. Further, a zoom-in on the point where the filter magnitude peaks is shown in Fig. 5b confirming stability. The peak gain value of 2.36 dB was measured at 3.86 kHz.

4 Conclusion

A fractional-order transfer function with fractional zeros and poles was proposed that approximates the magnitude ripple characteristics in the stopband of a inverse Chebyshev lowpass filter and maintains a fractional-order step in the transition from passband to stopband. The coefficients required for the ripple characteristics were determined using a least-squares fitting optimization routine. These fractional-order filters were realized using approximated fractional-order capacitors in a MIB circuit and were verified both simulation and with experimental results. This process has the potential to be expanded and applied to higher-order filters.

References

1. A. Acharya, S. Das, I. Pan, S. Das, Extending the concept of analog Butterworth filter for fractional order systems. Signal Process. **94**, 409–420 (2013)
2. P. Ahmadi, B. Maundy, A.S. Elwakil, L. Belostostski, High-quality factor asymmetric-slope band-pass filters: a fractional-order capacitor approach. IET Circuits Devices Syst. **6**(3), 187–197 (2012)
3. A.S. Ali, A.G. Radwan, A.M. Soliman, Fractional order Butterworth filter: active and passive realizations. IEEE J. Emerg. Sel. Top. Circuits Syst. **3**(3), 346–354 (2013)
4. A.M. Elshurafa, M.N. Almadhoun, K.N. Salama, H.N. Alshareef, Microscale electrostatic fractional capacitors using reduced graphene oxide percolated polymer composites, Appl. Phys. Lett. **102**(23), (2012). doi:10.1063/1.4809817
5. A.S. Elwakil, Fractional-order circuits and systems: an emerging interdisciplinary research area. IEEE Circuits Syst. Mag. **10**(4), 40–50 (2010)
6. T.J. Freeborn, B. Maundy, A.S. Elwakil, Approximated fractional-order Chebyshev lowpass filters. Math. Prob. Eng. (2015). doi:10.1155/2015/832468
7. T.J. Freeborn, B. Maundy, A.S. Elwakil, Field programmable analogue array implementations of fractional step filters. IET Circuits Devices Syst. **4**(6), 514–524 (2010)
8. T. Haba, G. Ablart, T. Camps, F. Olivie, Influence of the electrical parameters on the input impedance of a fractal structure realised on silicon. Chaos Solitons Fractals **24**(2), 479–490 (2005)

9. T. Helie, Simulation of fractional-order low-pass filters. IEEE/ACM Trans. Audio Speech Lang. Process. **22**(11), 1636–1647 (2014)
10. A. Marathe, B. Maundy, A.S. Elwakil, Design of fractional notch filter with asymmetric slopes and large values of notch magnitude. in *2013 Midwest Symposium Circuits Systems*, pp. 388–391 (2013)
11. B. Maundy, A.S. Elwakil, T.J. Freeborn, On the practical realization of higher-order filters with fractional stepping. Signal Process. **91**(3), 484–491 (2011)
12. A.G. Radwan, A.M. Soliman, A.S. Elwakil, First-order filters generalized to the fractional domain. J. Circuit Syst. Comput. **17**(1), 55–66 (2008)
13. A. Radwan, A. Elwakil, A. Soliman, On the generalization of second-order filters to the fractional-order domain. J. Circuit Syst. Comput. **18**(2), 361–386 (2009)
14. A. Radwan, A. Soliman, A. Elwakil, A. Sedeek, On the stability of linear systems with fractional-order elements. Chaos Solitons Fractals **40**(5), 2317–2328 (2009)
15. M. Sivarama Krishna, S. Das, K. Biswas, B. Goswami, Fabrication of a fractional order capacitor with desired specifications: a study on process identification and characterization. IEEE Trans. Electron. Devices **58**(11), 4067–4073 (2011)
16. A. Soltan, A.G. Radwan, A.M. Soliman, CCII based fractional filters of different orders. J. Adv. Res. **5**(2), 157–164 (2014)
17. A. Soltan, A.G. Radwan, A.M. Soliman, Fractional order Sallen–Key and KHN filters: stability and poles allocation. Circuits Syst. Signal Process. **34**(5), 1461–1480 (2015)
18. M.C. Tripathy, D. Mondal, K. Biswas, S. Sen, Experimental studies on realization of fractional inductors and fractional-order bandpass filters. Int. J. Circuit Theory Appl. **43**(9), 1183–1196 (2015)
19. G. Tsirimokou, C. Laoudias, C. Psychalinos, 0.5-V fractional-order companding filters. Int. J. Circuit Theory Appl. **43**(9), 1105–1126 (2015)